Magnetic phase diagram of $Sn_{1-x}Mn_xTe$ epitaxial layers

M. Zięba[1], K. Gas[1], A. Grochot[1], K. Dybko[1,2], A. Kazakov[2], V.V. Volobuev[2], B. Turowski[2], W. Zaleszczyk[1,2], W. Wołkanowicz[1], A. Reszka[1], R. Minikayev[1], T. Wojciechowski[1,2], H. Przybylińska[1], M. Sawicki[1], T. Wojtowicz[2], T. Story[1,2]

[1] Institute of Physics, Polish Academy of Sciences, Warsaw, Poland

[2] International Research Centre MagTop, Institute of Physics, Polish Academy of Sciences, Warsaw, Poland

Introduction

- $Sn_{1-x}Mn_xTe$ is a IV-VI semimagnetic (diluted magnetic) semiconductor known to exhibit both the properties of topological crystalline insulators (TCI) and carrier – induced ferromagnetism. The incorporation of magnetic ions (Mn^{2+}) into host matrix turns $Sn_{1-x}Mn_xTe$ into a ferromagnet at helium temperatures. Here the magnetic properties depends not only on manganese content but also on concentration of carriers due to long – range RKKY exchange interactions [4].
- To fully exploit this unique physical regime we carried out technological program of molecular beam epitaxial growth of $Sn_{1-x}Mn_xTe$ ($x \le 0.1$) layers on various crystalline substrates and experimental studies of the dependence of their magnetic, structural, and electric properties on Mn content, carrier concentration and crystal deformation.

RKKY exchange interaction

- The RKKY is a long – range indirect exchange interaction mediated by the free carriers. In $Sn_{1-x}Mn_xTe$ density of carriers depends on number of cation vacancies (one Sn vacancy produces 2 charge carriers – holes).
- The band structure of the compound is of great importance due to presence of the second valence band located along Σ – line in the Brillouin Zone, characterized by much higher effective masses of the carriers than in the main valence band at L point. When the Fermi level enters the band of the heavy holes ($p_c = 3 \times 10^{20}$ cm^{-3}) the strength of the interaction becomes strongly enhanced thus inducing ferromagnetic state.

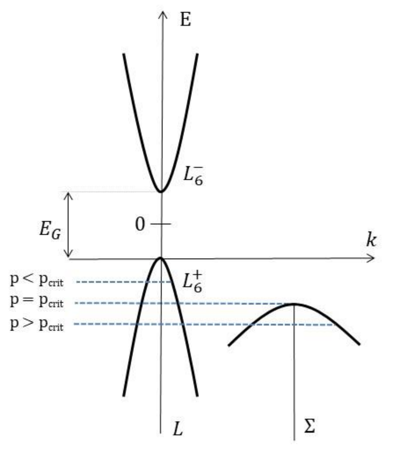

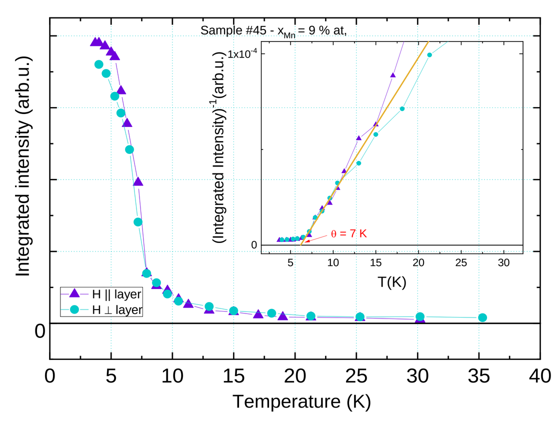

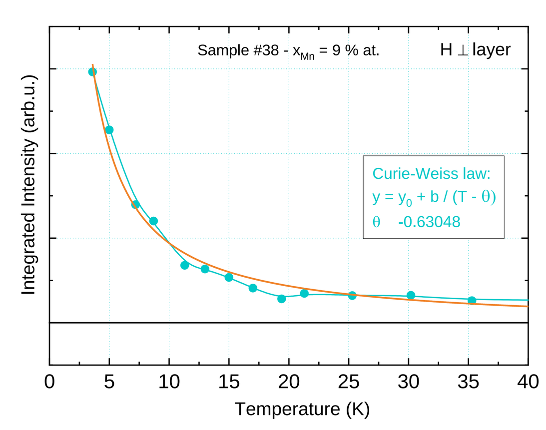

- The role of carriers in the RKKY exchange interaction is presented for two samples with equal Mn content:
  - Sample #45 with carrier concentration $p = 1 \times 10^{21}$ cm^{-3} – ferromagnetic state with Curie temperature T_C = 8 K
  - Sample #38 with carrier concentration $p = 2 \times 10^{20}$ cm^{-3} – paramagnetic state described by Curie – Weiss law

Preparation of Samples and Their Characterization

- Thin films of thickness within the range 0.3 – 1.5 µm were grown by molecular beam epitaxy (MBE) using BaF_2(111), BaF_2 (001) and CdTe/GaAs (001) substrates.
- The Samples were grown using SnTe, Mn, Te effusion cells to vary both Mn content and carriers concentration. Additional Cd source were used to refresh CdTe buffer layer on GaAs (001) substrate.
- Additional buffer layers of SnTe were deposited in order to decrease lattice mismatch and to accommodate the strain between substrate and primary $Sn_{1-x}Mn_xTe$ layer.
- The X-ray diffraction analysis of the layers on three types of the substrates revealed the expected growth direction and the rock-salt crystal structure for each sample.

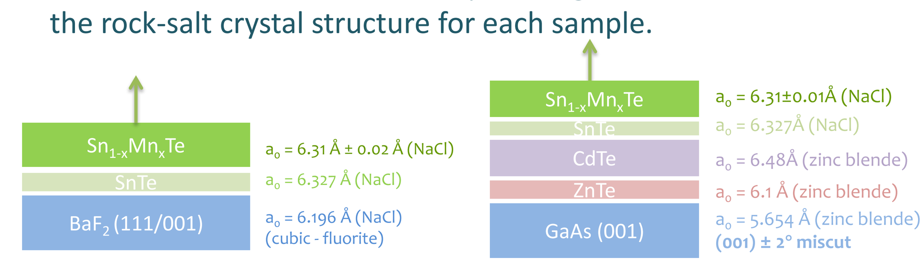

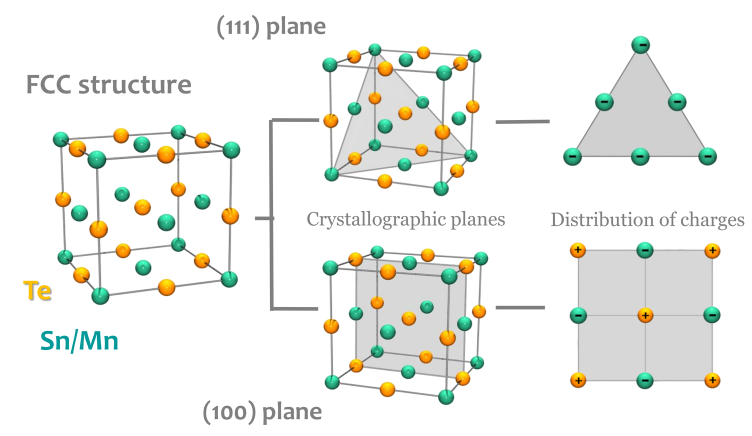

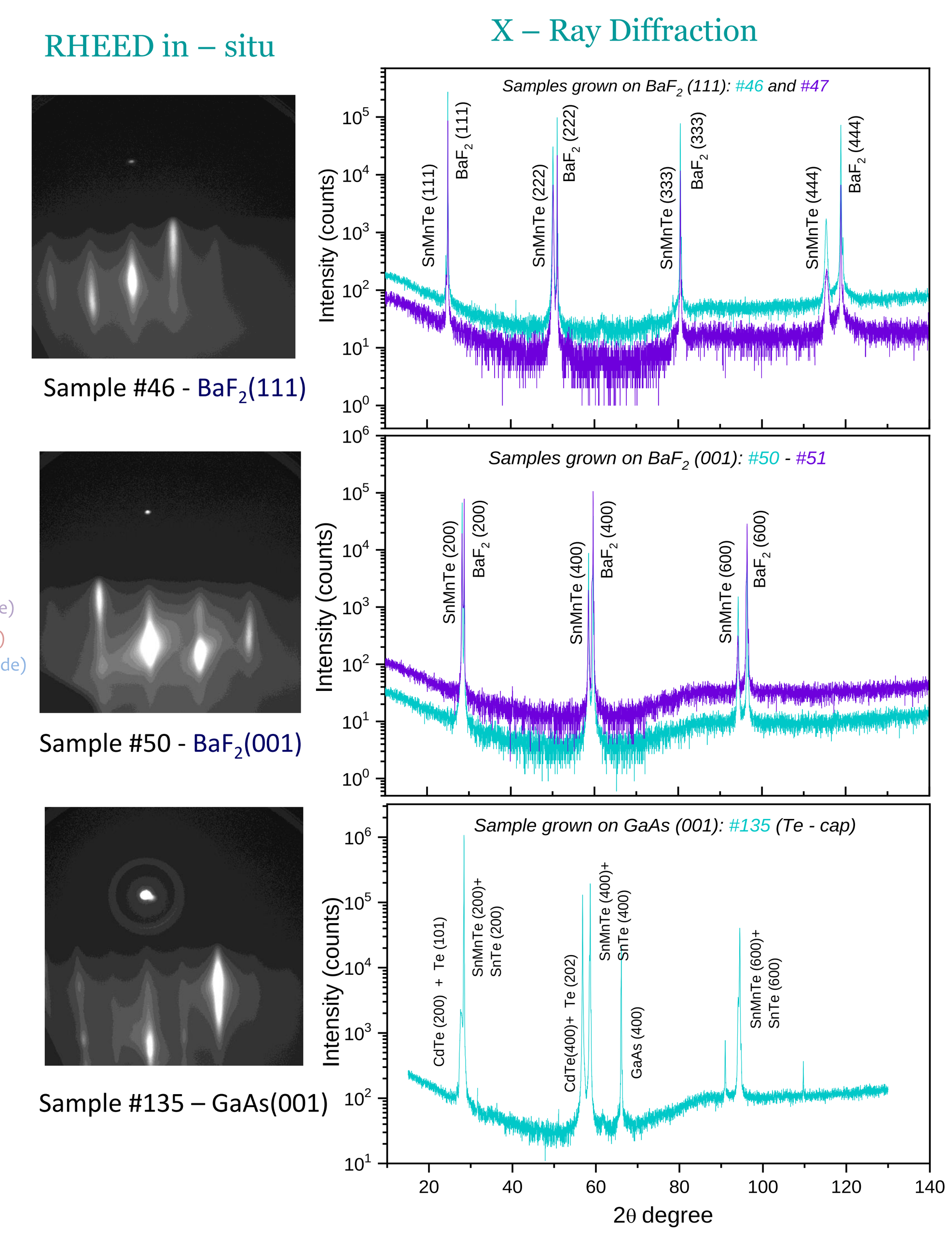

Magnetization saturation

- M(H) measurements for exemplary samples corrected for the diamagnetic signal from substrate BaF_2 as determined experimentally at 300 K, where the paramagnetic contribution of the layer can be neglected.
- All the samples exhibit a lower magnetization saturation than expected for fully saturated (T= 0 K) system with nominal content (confirmed by EDX) of Mn^{2+} ions with S = 5/2 ($M_S = N*5\mu_B$). Carrier concentration for all presented samples fit in the range 5×10^{20} cm$^{-3} \le p \le 9 \times 10^{20}$ cm^{-3}.

Magnetization saturation for epilayers on various substrates:

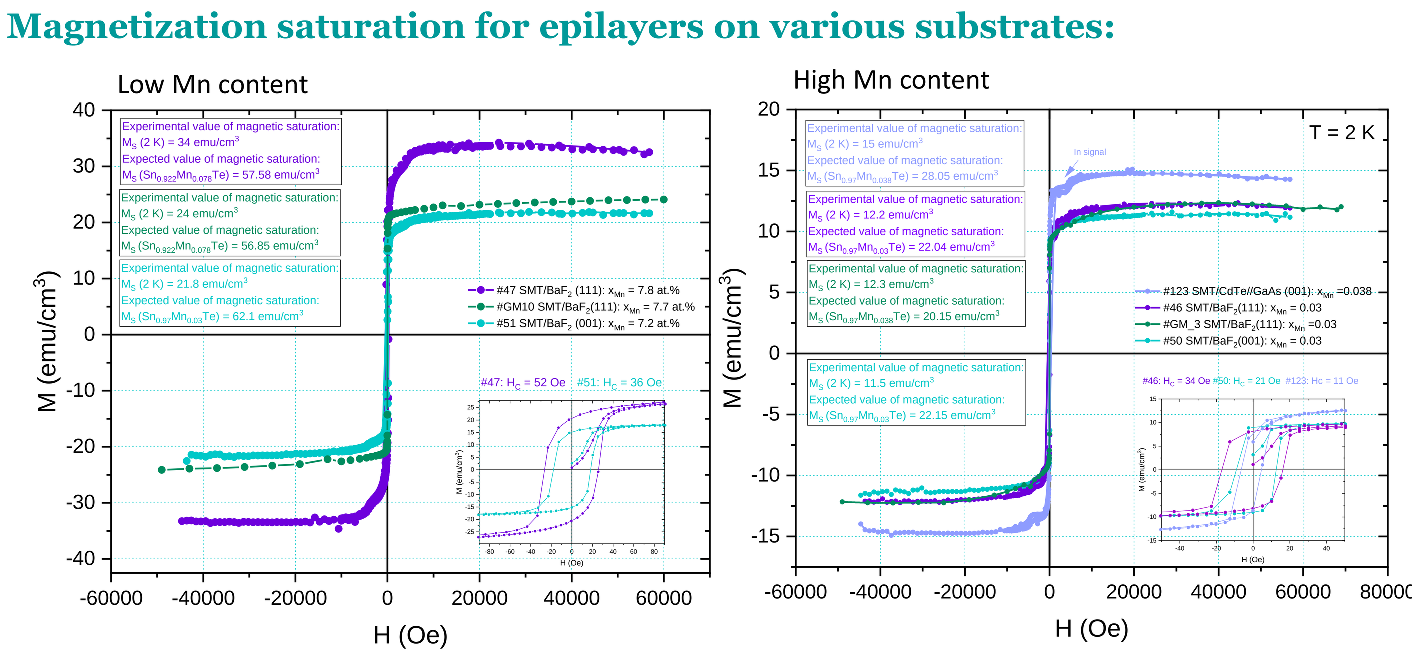

Nr	Substrate	X	M_S (experimental)	M_S (calculated)	Saturation
#47	BaF_2 (111)	0.078	34.0 emu/cm³	57.6 emu/cm³	60%
#GM10	BaF_2 (111)	0.077	24.0 emu/cm³	56.9 emu/cm³	42%
#51	BaF_2 (001)	0.072	21.8 emu/cm³	53.2 emu/cm³	41%
#123	CdTe/GaAs(001)	0.038	15.0 emu/cm³	28.5 emu/cm³	53%
#GM3	BaF_2 (111)	0.03	12.3 emu/cm³	20.2 emu/cm³	61%
#46	BaF_2 (111)	0.03	12.2 emu/cm³	22.4 emu/cm³	55%
#50	BaF_2 (001)	0.03	11.5 emu/cm³	20.2 emu/cm³	57%

Magnetization saturation for various x content:

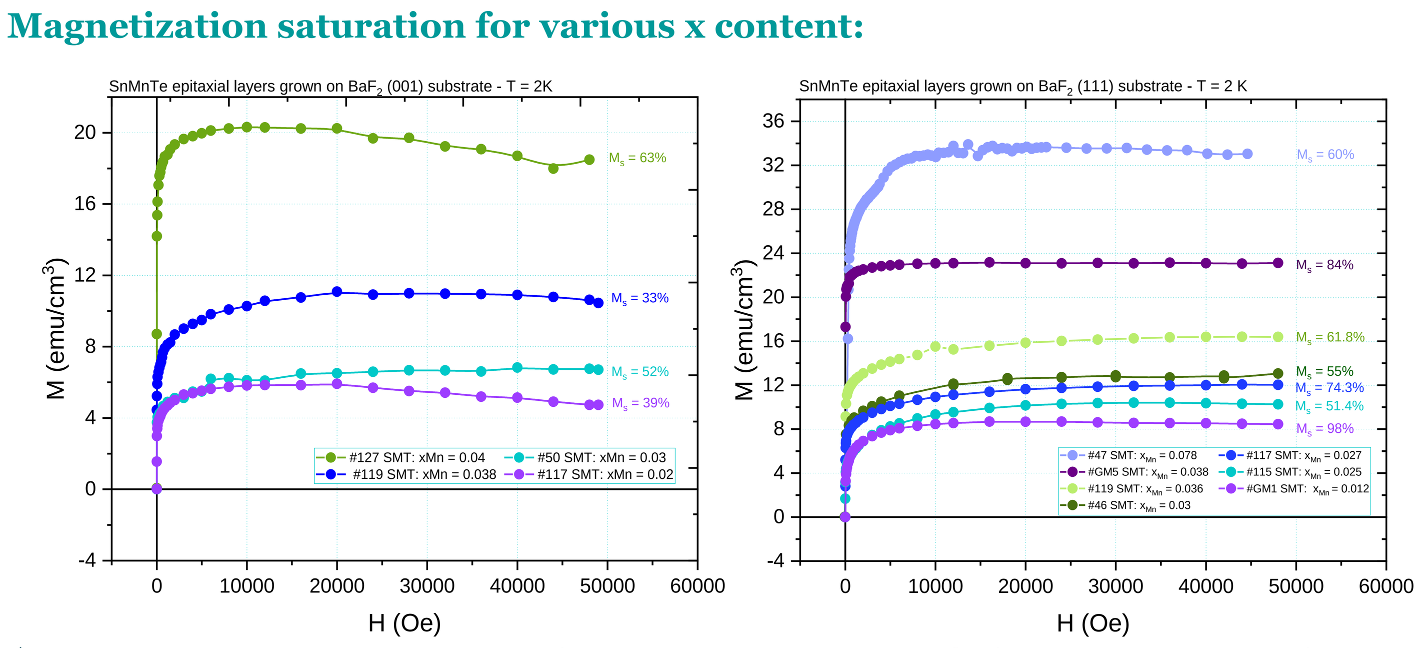

- Magnetization saturation increases with increasing Mn composition for layers grown on BaF_2 substrates and it's higher for epitaxial layers with smaller ($x \le 0.04$) manganese content.
- The magnetic field dependence of the magnetization for few samples shows gradual increase of the magnetization even at higher fields.

Determining Curie Temperature

- The Curie temperature was estimated from the temperature dependence of the thermoremanent magnetization (TRM) at field H ≈ 0 Oe while warming the sample, after field cooling (FC) down to T = 2 K at magnetic field H = 0.1 – 1 kOe. Curie temperature is defined by the point where the TRM signal reaches zero.
- Values of T_C (TRM) obtained from SQUID are with good agreement with T_C determined from temperature dependence of FMR signal.

Curie Temperatures for various manganese content (x):

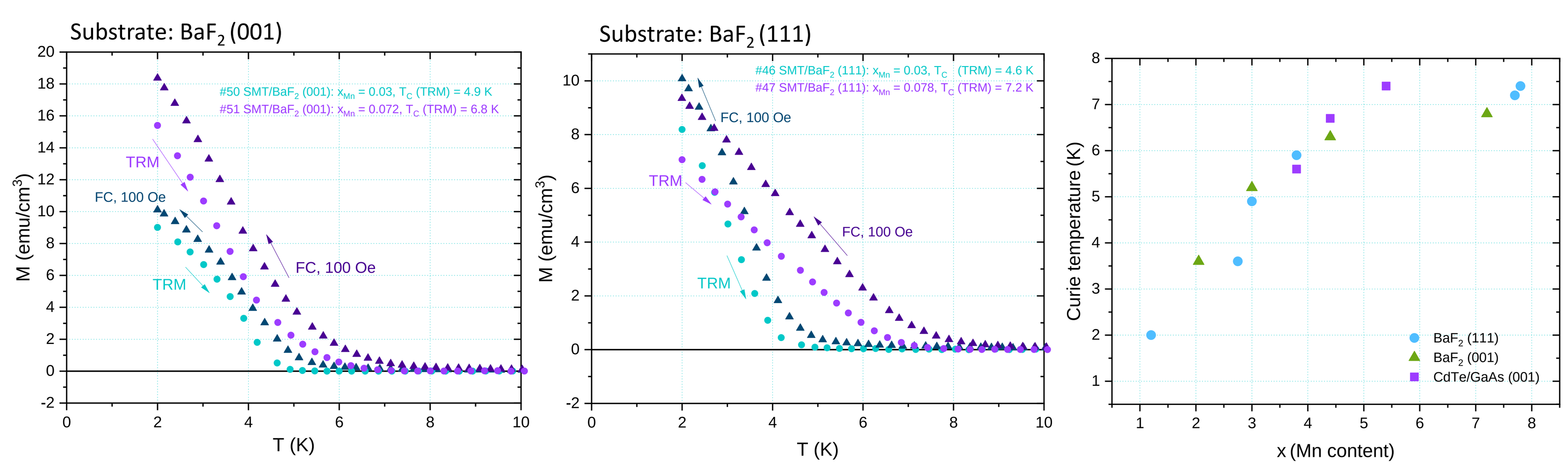

Temperature dependence of FMR signal

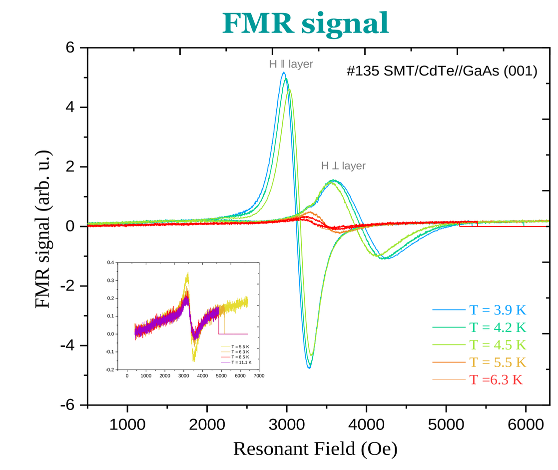

Magnetic anisotropy

- The analysis of the angular dependence of the FMR resonance field revealed a dominant magnetic shape anisotropy contribution for all investigated layers with easy magnetization axis located in the plane of the layer. However, while all (001) oriented layers were found to exhibit perfect cubic symmetry, those grown on BaF_2 (111) substrate reveal in angular dependence of FMR resonant field the linewidth features characteristic of material with rhombohedral distortion along the [111] growth direction.
- Such distortion is known in SnTe and GeTe-based crystals. In contrast to closely related GeMnTe layers, where such crystal distortion induces perpendicular magnetic anisotropy [3], in $Sn_{1-x}Mn_xTe$ layers in all the substrates studied the easy direction of magnetization remains in the plane of the layer.

FMR resonant field and linewidth as a function of the direction of the external magnetic field

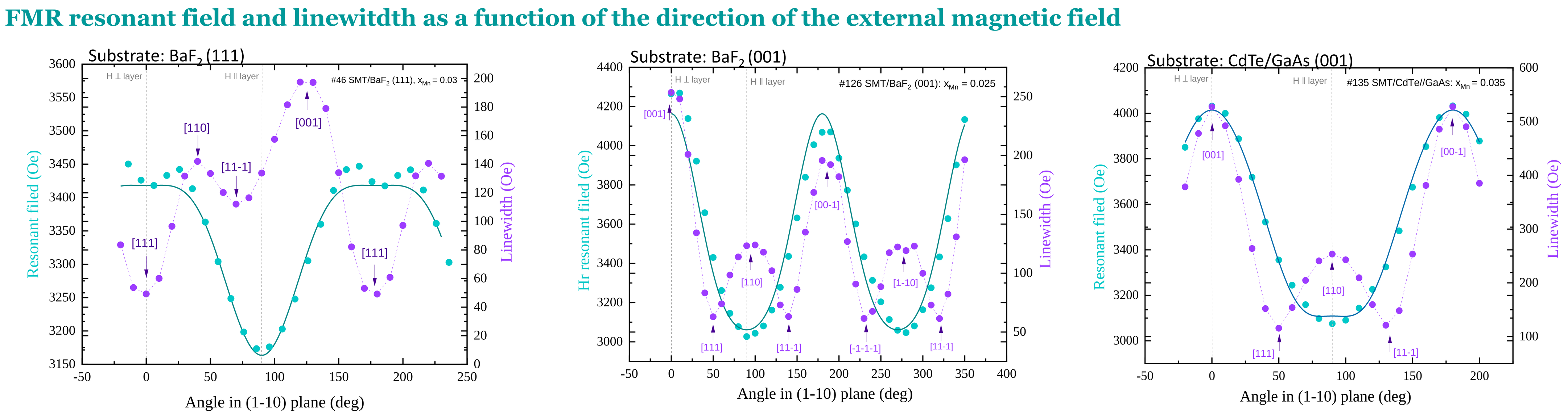

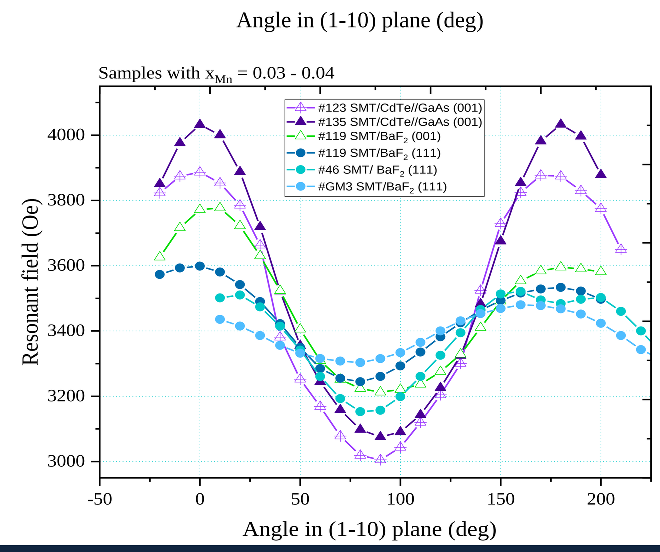

- The contributions to the magnetic anisotropy in the $Sn_{1-x}Mn_xTe$ epitaxial layers arise from:
  - Shape anisotropy (dipolar)
  - Single – ion crystalline anisotropy (cubic)
  - Single – ion crystalline anisotropy (tetragonal)
- The quantitative analysis of anisotropy constants is based on angular dependence of FMR resonant field.

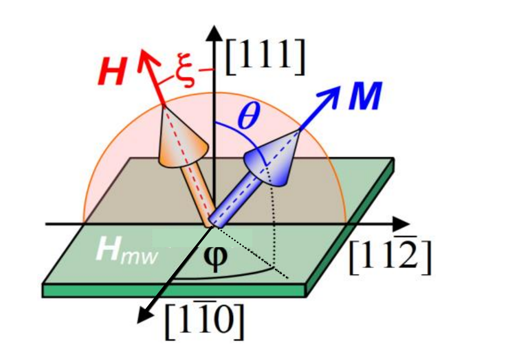

Geometry of the FMR measuring system

Conculsions - Magnetic phase diagram

- The carrier concentration dependence of the normalized Curie – Weiss temperature of $Sn_{1-x}Mn_xTe$ and $Pb_{1-x-y}Sn_yMn_xTe$ bulk crystals (black points) and $Sn_{1-x}Mn_xTe$ epitaxial layers (blue – grown by V. Volobuev, orange – grown by A. Nadolny, green – grown by R. Adhikari and turquoise – grown by M. Zięba). The solid line (gray) is the result of theoretical calculations based on the RKKY interaction due to both the light (L-band) and the heavy (Σ-band) holes [1].

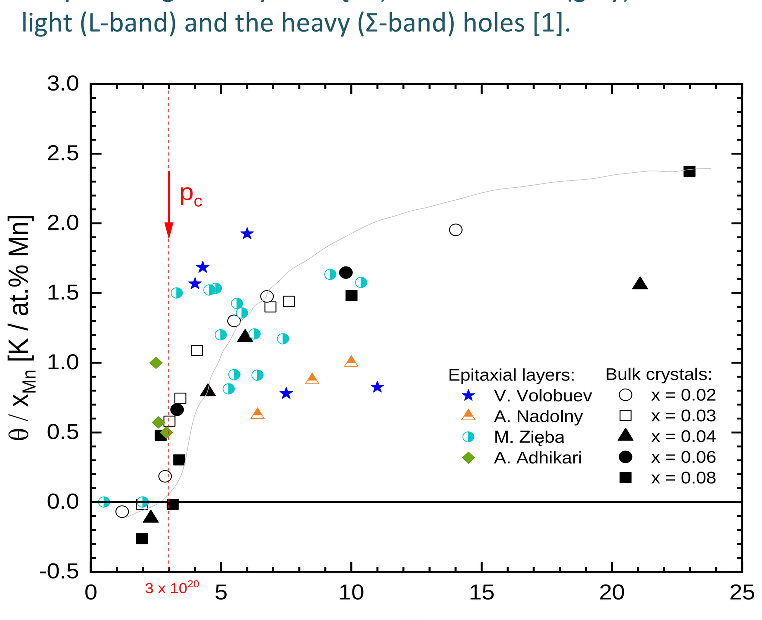

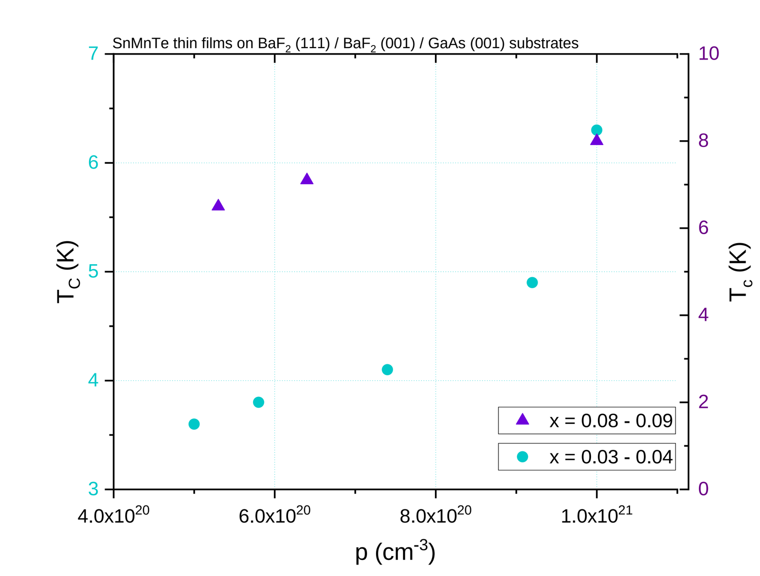

Carrier – Induced Ferromagnetism in $Sn_{1-x}Mn_xTe$ epitaxial layers

- We grew a series of $Sn_{1-x}Mn_xTe$ (0.03 < x < 0.08) epitaxial layers on BaF_2 (111), BaF_2 (001) and CdTe/GaAs (001) substrates.
- We found that in $Sn_{1-x}Mn_xTe$ ($0.03 \le x \le 0.084$) layers, even for the highest Mn content studied and optimal hole concentration, the ferromagnetic transition temperature is below T_C < 10 K, i.e., about twice smaller than in corresponding bulk crystals [1]. It indicates that in our optimal growth regime the substitution of Mn ions at cation sites of the rock-salt lattice of SnTe is limited [2].
- FMR studies of magnetic anisotropy confirm in-plane easy magnetization axis in $Sn_{1-x}Mn_xTe$ layers on both substrates.

References & Acknowledgments

[1] P.J.T. Eggenkamp et al., Phys. Rev. B **51, 15250 (1995).**
[2] A. Nadolny, et al., J. Magn.Magn. Mat. **248, 134 (2002).**
[3] H. Przybylińska et al., Phys. Rev. Lett.**112, 047202 (2014).**
[4] R. Adhikari et al., Phys. Rev. B **100, 134422 (2019).**
[5] A. Sulich et al., J. Mater. Chem. C **10, 3139-3152 (2022);** poster presentation at this conference.
[6] A. Kazakov et al. Poster presentation at this conference.

This research was partially supported by the Foundation for Polish Science through the IRA Programme co-financed by EU within SG OP and by the NCN Grant: UMO 2017/27/B/ST3/02470

European Union European Regional Development Fund · European Funds Smart Growth · Republic of Poland · FNP Foundation for Polish Science · Narodowe Centrum Nauki